

Proceedings of the 2017 Summer Biomechanics, Bioengineering, and Biotransport Conference

June 21 – 24, 2017 Tucson, AZ

SBC³

biomechanics.
bioengineering.
biotransport.

This is an electronically searchable and linked version of the program.

Instructions for abstract search:

1) Click on abstract title in Session Listing
or

2) Search by keyword or author using find option:

[control] + F (PC)

[command] + F (Mac)

PREDICTION OF POST STENOTIC FLOW INSTABILITIES IN A PATIENT SPECIFIC COMMON CAROTID ARTERY MODEL

Mancini V. (1), Bergersen A. (2), Segers P. (1), Valen-Sendstad K. (2)

(1) IBiTech - bioMMeda
Ghent University
9000 Ghent, Belgium

(2) Scientific Computing
Simula Research Laboratory
1325 Lysaker, Norway

INTRODUCTION

In silico medicine shows great potential for revealing mechanisms of atherosclerotic plaque progression in the carotid bifurcation by modelling patient-specific local hemodynamic forces [1]. It is well known that the pulsatile nature of the flow in combination with narrowing of the lumen can cause post stenotic flow instabilities, which presents additional challenges from a flow modelling point of view. The three most common modelling approaches for unstable or turbulent flows are Reynolds-averaged Navier-Stokes (RANS), large eddy simulation (LES), and direct numerical simulation (DNS). RANS is the computationally cheapest one, but has shown to be directly misleading for predicting transitional flows [2]. DNS is in contrast accurate, but on the other hand extremely computationally expensive. LES can potentially offer an ideal balance between accuracy and computational cost [3]. The aim of this study was to explore the parameter space of the numerical simulation, and establish a DNS reference solution for stenotic carotid bifurcation, and that will be used in the future to assess whether LES can accurately predict post stenotic flow instabilities.

METHODS

Medical images of a carotid bifurcation with severe stenosis (82% by area) located in the internal carotid artery (ICA) of a 75 years old man were obtained from computed tomography angiography and segmented using *3D Slicer* [4]. The *Vascular Modelling Tool Kit* was used to create meshes with a local refinement in the stenotic- and downstream region, resulting in meshes ranging from 2 to 50 million (M) linear tetrahedral cells. Flow simulations were performed using the open-source CFD solver *Oasis* [5], where special care was taken to ensure a kinetic energy preserving and minimally dissipative numerical solution. The fluid was set to mimic water with kinematic viscosity of $\nu = 1 \cdot 10^{-6} \text{ m}^2/\text{s}$, and a Reynolds number was 1400 at the inlet, to

allow for direct comparison with *in vitro* experiments at a later point. The flow field was evaluated at peak systolic flow rate of 585.52 ml/min, thus, enabling rigorous assessment of the temporal and spatial resolution with respect to the smallest scales, however at the cost of an artificial flow condition. A parabolic velocity profile was prescribed as inlet condition, no-slip along the walls, and a resistance condition to meet a flow split between the ICA and the external carotid artery at 68.2:31.8, to obtain physiologically plausible flow split [6]. The initial condition was a fully developed flow from the 2M simulation that was projected onto each mesh.

We performed a spatial refinement study to obtain a reference solution, with a fixed time step (Δt) of $2 \cdot 10^{-5} \text{ s}$. Using the least computationally expensive mesh that gave adequate results, a temporal refinement study was performed, with Δt ranging from $1 \cdot 10^{-4}$ to $5 \cdot 10^{-6} \text{ s}$.

The instantaneous velocity (u) was decomposed into the mean (\bar{u}), and fluctuating components (u'), respectively ($u = \bar{u} + u'$), to compute the turbulent kinetic energy (TKE) $k = 0.5(u'^2 + v'^2 + w'^2)$. The analyses were based on the time interval from 0.1 to 2.0 s, to allow for initial transients to wash out and statistics to converge. Figure 1 (left) shows the region of interest and four cut planes (A to D) where we computed the time-averaged velocity. In addition, the power spectral density (PSD) of u' downstream of the stenosis (point P in Figure 1) was computed by using the Welch method with Hann windowing with data from 0.1 to 0.5 s.

RESULTS

Focusing first of qualitative results, Figure 1 (right) shows the volumetric TKE for the 22M simulation, and we can clearly observe flow instabilities already upstream of the stenosis, which increases in

intensity at the center and downstream of the stenosis. However, the flow instabilities quickly dissipate further downstream.

The time-averaged velocity is shown in cut planes A to D from the spatial and temporal refinement study in Figure 2, left and right respectively. The 22M mesh was found to offer an optimal balance between accuracy and computational cost: the time-averaged velocity obtained from the finest 50M mesh are comparable with the 22M mesh, whereas it differs for the 2M and 6M simulation. Therefore, the 22M mesh was used for the temporal refinement study.

From the time-averaged velocity in Figure 2 (right) we find that the three largest time steps are phenotypically similar, although the smallest time steps show large differences, in particular at C1-C2.

The spectral distribution of energy in Figure 3 (left) confirms the ability of the 22M to sufficiently replicate the finest mesh results. Furthermore, from Figure 3 (right) we can observe adequate agreement between the different temporal resolutions.

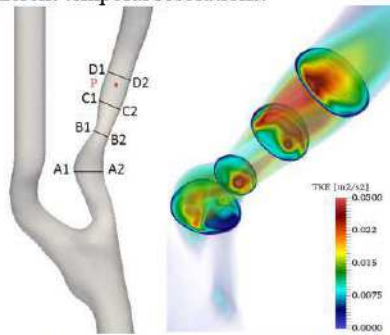


Figure 1: Region of interest with planes A to D and point P (left), and a volume rendering of the TKE and in planes A to D (right).

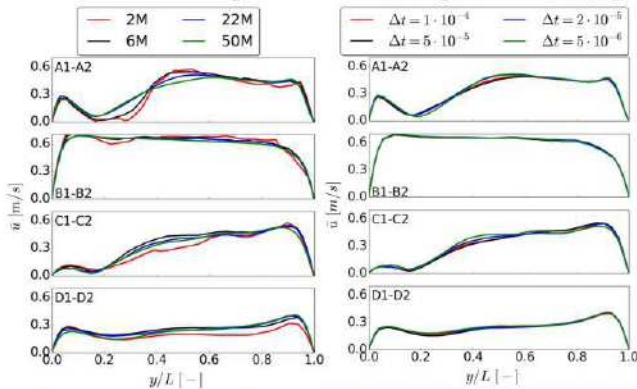


Figure 2: Time-averaged velocity along the four lines of interest for the spatial (left) and temporal (right) refinement study.

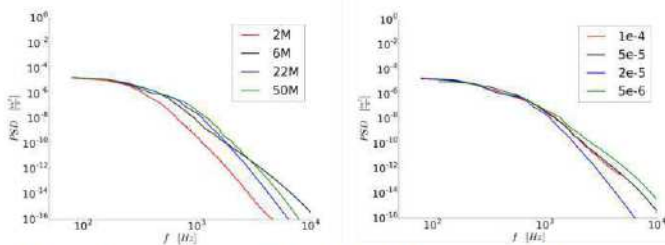


Figure 3: Power spectral density of the velocity field at point P, located 1.7 cm (2.2 diameters) downstream of the stenosis.

DISCUSSION

The aim of this study was to explore the parameter space relative to a DNS reference solution, a 22M mesh with a time step of $1 \cdot 10^{-4}$ s

was found to be an optimal choice between computational cost and accuracy, and will be used in future studies on turbulence modeling for stenotic carotid bifurcations. That being said, there is admittedly a minor difference between 22M and 50M in Figure 2 (left). To assess if the 50M simulation was close enough to a proper DNS we compared the temporal (Δt) and spatial (Δx) scales in the numerical simulation to the Kolmogorov time scale (τ), and length scale (η), respectively.

The results of spatial assessment can be found in Table 1, displaying the mean Δx , the smallest Kolmogorov length scale, and the maximum ratio. There are two things of note, *first* the Kolmogorov length scale converges as the mesh is refined. *Second*, the ratio of the two finest meshes are below 10, typically sufficient to capture > 95 % of the dissipation. If the simulations, from a numerical point of view, were truly converged, the ratio needs to be unity. However, as observed in bottom right of Table 1, that would require a mesh with $\sim 7^3$ times 50M cells, if uniformly refined. We therefore consider the 50M sufficiently refined from a pragmatic point of view, and by extension the 22M mesh for biomedical applications. Furthermore, the difference in CPU hours is substantial, the 22M simulation with $\Delta t = 1 \cdot 10^{-4}$ used 1420 CPU hours on 96 cores, while the 50M simulation with $\Delta t = 2 \cdot 10^{-5}$ s spent 16 496 CPU hours on 128 cores to simulate 2 physical seconds, over an 11-fold difference.

Table 1: Comparison between Kolmogorov length scale and Δx

Num. of cells	2M	6M	22M	50M
Δx_{mean} [m]	3.19E-4	2.14E-4	1.38E-4	1.05E-4
η_{min} [m]	9.81E-6	9.30E-6	8.91E-6	8.58E-6
$(\Delta x/\eta)_{max}$ [-]	21.93	14.04	9.31	7.49

The temporal assessment of the flow simulation can be found in Table 2, showing that the temporal resolution was below the Kolmogorov scales. Furthermore, we can observe from the PSD in Figure 3 (left) that there was, for all practical purposes, no energy in the fluctuating component above 5000 Hz. We can therefore attribute the discrepancies observed in Figure 2 (lower) to an inadequate data for time-averaging (0 – 0.7 s). In fact, an even larger time step might have been an adequate temporal resolution, however $\Delta t = 1 \cdot 10^{-4}$ s is very close to the stability criteria of the solver.

Table 2: Comparison between Kolmogorov time scale and Δt

Δt [s]	1.00E-4	5.00E-5	2.00E-5	5.00E-6
τ_{min} [s]	7.96E-5	7.96E-5	7.93E-5	7.92E-5
$\Delta t/\tau_{min}$ [-]	1.2563	0.6281	0.2522	0.0631

The simulations were performed with rigid walls, and the effect of a compliant model remains to be assessed. Furthermore, the fluid used for these simulations was water instead of blood to allow for direct comparison against *in vitro* experiments, which will be the focus of future work. As part of a larger consortium, the final aim of this line of investigation is to build a non-contact device to diagnose severe stenosis in the carotid arteries through the analysis of neck's skin displacement. We will therefore compute the sensitivity of the flow split and of noise in the inflow pulse through *in silico* experiments, since both factors can be challenging to control in the *in vitro* experiments.

ACKNOWLEDGEMENTS

Funding: EU Horizon 2020 programme (CARDIS; ICT-26-2014).

REFERENCES

- [1] Steinman DA. et al., *Annals of Biomed Eng.*, 30:483-497 2002.
- [2] Varghese S. et al., *J. Fluid Mech.*, 582:281-318, 2007.
- [3] Aspden A. et al., *Commun Appl Math Comput Sci*, 3:103-26, 2009.
- [4] Iannaccone F. et al., *Int J Art Org.*, 37: 928-939, 2014.
- [5] Mortensen M. et al., *Comp Phys Comm*, 188:177-188, 2015.
- [6] Groen H. C. et al., *J Biomechs*, 43: 2332-8, 2010.